JACS
JOURNAL OF THE AMERICAN CHEMICAL SOCIETY
Article
pubs.acs.org/JACS

Mechanism of Metal-Free Hydrogen Transfer between Amine–Boranes and Aminoboranes

Erin M. Leitao, Naomi E. Stubbs, Alasdair P. M. Robertson, Holger Helten,† Robert J. Cox, Guy C. Lloyd-Jones,* and Ian Manners*

School of Chemistry, Cantock's Close, University of Bristol, Bristol BS8 1TS, United Kingdom

Supporting Information

ABSTRACT: The kinetics of the metal-free hydrogen transfer from amine–borane $Me_2NH{\cdot}BH_3$ to aminoborane $iPr_2N{=}BH_2$, yielding $iPr_2NH{\cdot}BH_3$ and cyclodiborazane $[Me_2N\text{-}BH_2]_2$ via transient $Me_2N{=}BH_2$, have been investigated in detail, with further information derived from isotopic labeling and DFT computations. The approach of the system toward equilibrium was monitored in both directions by $^{11}B\{^1H\}$ NMR spectroscopy in a range of solvents and at variable temperatures in THF. Simulation of the resulting temporal–concentration data according to a simple two-stage hydrogen transfer/dimerization process yielded the rate constants and thermodynamic parameters attending both equilibria. At ambient temperature, the bimolecular hydrogen transfer is slightly endergonic in the forward direction ($\Delta G_1^\circ{}_{(295)}$ = 10 ± 7 kJ·mol^{-1}; $\Delta G_1^{\ddagger}{}_{(295)}$ = 91 ± 5 kJ·mol^{-1}), with the overall equilibrium being driven forward by the subsequent exergonic dimerization of the aminoborane $Me_2N{=}BH_2$ ($\Delta G_2^\circ{}_{(295)}$ = −28 ± 14 kJ·mol^{-1}). Systematic deuterium labeling of the NH and BH moieties in $Me_2NH{\cdot}BH_3$ and $iPr_2N{=}BH_2$ allowed the kinetic isotope effects (KIEs) attending the hydrogen transfer to be determined. A small inverse KIE at boron (k_H/k_D = 0.9 ± 0.2) and a large normal KIE at nitrogen (k_H/k_D = 6.7 ± 0.9) are consistent with either a pre-equilibrium involving a B-to-B hydrogen transfer or a concerted but asynchronous hydrogen transfer via a cyclic six-membered transition state in which the B-to-B hydrogen transfer is highly advanced. DFT calculations are fully consistent with a concerted but asynchronous process.

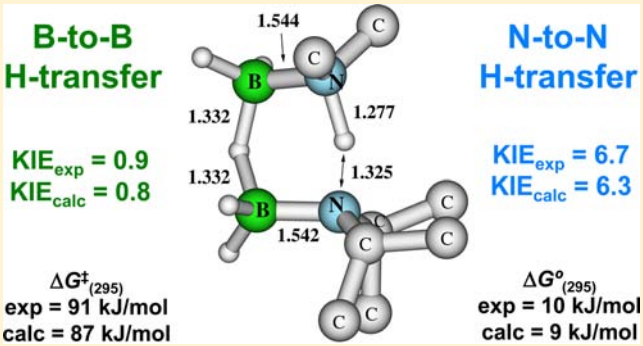

INTRODUCTION

Amine–boranes, $R_3N{\cdot}BR'_3$, and aminoboranes, $R_2N{=}BR'_2$ (R, R′ = H, alkyl, aryl), represent two of the simplest and most studied classes of inorganic molecules. These compounds, along with related boron–nitrogen species, have played a key role in the development of inorganic chemistry due to their isostructural and isoelectronic relationship to well-known organic compounds.[1−8] Amine–boranes are also important as reagents and are widely utilized as hydroboration agents for organic substrates and for the reduction of metal salts to generate metal nanoparticles.[9] In this respect, their easy handling and increased stability has led to a valuable role as mild and convenient alternatives to commercial borane reagents $L{\cdot}BH_3$ (L = THF or SMe_2).

As a result of the growing need for the development of sustainable and environmentally benign alternatives to petroleum and other fossil fuels, there has been a surge of interest in amine–boranes over the past decade.[10−18] In this context, ammonia–borane, $NH_3{\cdot}BH_3$, an air-stable solid with a hydrogen content of 19.6%, has attracted much attention as a possible alternative to liquid hydrogen as a portable hydrogen storage material.[11] For this to be realistic, the facile release of hydrogen and rehydrogenation of the resulting spent fuel is necessary.[6,14,18−20]

Amine–borane dehydrogenation chemistry is also of interest as a route to polyaminoboranes, $[RNH\text{-}BH_2]_n$, boron–nitrogen analogues of polyolefins, and "white graphene", single-layer films of hexagonal boron nitride.[7,21−25] Furthermore, inspired by the broad interest in amine–borane dehydrogenation, an emerging field of amine–borane and aminoborane coordination chemistry is now attracting much attention.[26−32] Elimination of hydrogen from amine–boranes was first established thermally (>100 °C; extended periods);[33−36] more recently, it has been shown to proceed very efficiently at lower temperatures under catalytic conditions. A wide range of catalysts has been reported for amine–borane dehydrogenation, based mainly on transition metals[2,37−49] but also, in several cases, main-group elements[50−54] (eq 1).

$$\underset{\text{R, R' = H, alkyl, aryl}}{RR'NH{\cdot}BH_3} \xrightarrow[-\,H_2]{\text{catalyst}} {}^1/_x\,[RR'N\text{-}BH_2]_x \qquad \underset{x = 1, 2, 3\ldots > 150{,}000}{} \qquad (1)$$

Using Ir, Ru, Fe, Ni, and Rh catalysts, the dehydropolymerization of monoalkylamine–boranes (e.g., $MeNH_2{\cdot}BH_3$,

Received: July 27, 2012
Published: September 27, 2012

   dx.doi.org/10.1021/ja307247g | J. Am. Chem. Soc. 2012, 134, 16805−16816

*n*BuNH$_2$·BH$_3$) and NH$_3$·BH$_3$ can be achieved by the controlled elimination of 1 equiv of H$_2$.[37,45,55,56] In the case of Ir, preliminary studies suggest that the initial product of dehydrogenation may be a transient aminoborane (RNH═BH$_2$, R = H, Me, *n*Bu), which subsequently polymerizes at the metal center to give poly(alkylaminoboranes)[21,37] (Scheme 1).

Scheme 1. Metal-Mediated Amine−Borane Dehydropolymerization[37]

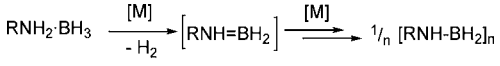

R = H, Me, *n*Bu; [M] = catalyst

We recently reported the discovery that aminoboranes function as hydrogen acceptors to allow the metal-free dehydrogenation of several amine−boranes at ambient temperatures (eq 2).[50]

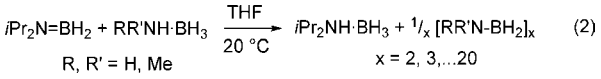

(2)

Interestingly, when R = R′ = Me, the reaction proceeded much more cleanly (eq 3) than when R′ = Me, R = H or R = R′ = H, where [H$_2$B(μ-H)(μ-NRR′)BH$_2$] is a major side product (eq 4). In contrast, the undetected aminoborane Me$_2$N═BH$_2$, presumed to be formed after hydrogen transfer, spontaneously dimerized to generate the well-known cyclodiborazane, [Me$_2$N-BH$_2$]$_2$.[40,57]

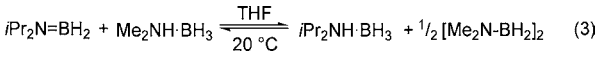

(3)

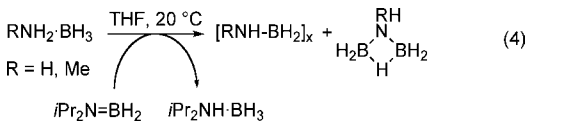

(4)

This result was significant as, to the best of our knowledge, direct hydrogenation of aminoboranes had not been previously reported.[20] Moreover, the ability to hydrogenate formally unsaturated boron−nitrogen species is relevant to the problem of regeneration of spent fuels in hydrogen storage applications. In addition, the hydrogen transfer reaction between amine−boranes and aminoboranes offers the potential for the formation of metal-free oligomers and/or polymers in the absence of a catalyst, as was observed with hydrogen transfer from the amine−borane adducts MeNH$_2$·BH$_3$ and NH$_3$·BH$_3$ by ^{11}B NMR spectroscopy (eq 4).[50] The hydrogen transfer reactivity is also highly relevant with respect to the mechanistic considerations associated with metal-catalyzed group 13−15 dehydrocoupling reactions as, to date, the focus has been almost entirely on the role of the metal.

This hydrogen transfer chemistry can also be considered within the context of recent work on metal-free transfer hydrogenation reactions of organic substrates. For example, alkenes,[58] ketones,[59−61] aldehydes,[62,63] ketimines, quinolines,[64−66] and N-heterocycles can be hydrogenated by employing various protic acids in combination with formal hydride sources, such as Hantzsch esters.[67−69] A further recent advance is the use of frustrated Lewis pair (FLP) systems such as *i*Pr$_2$NH and the Lewis acid B(C$_6$F$_5$)$_3$ to enable the catalytic hydrogenation of substrates such as imines.[70−72] A related example is reversible hydrogen activation by *ansa*-aminoboranes, which can be utilized to hydrogenate silyl enol ethers.[73,74] Berke and co-workers have also recently reported stoichiometric metal-free hydrogenations of organics using NH$_3$·BH$_3$ as the source of hydrogen, a process that has been applied to the reduction of polar olefins,[75] imines,[51] aldehydes, and ketones.[76] Similarly, Musgrave and co-workers have suggested computationally the metal-free hydrogenation of carbon dioxide with NH$_3$·BH$_3$.[77,78]

A detailed understanding of hydrogen transfer chemistry between amine−boranes and aminoboranes will be essential for the effective development of aminoborane hydrogenation. In addition to direct utility, mechanistic insight will also be relevant for controlling hydrogen transfer in, e.g., dehydrocoupling reactions. Herein we report on a detailed kinetic and computational investigation of the equilibrium hydrogen transfer between Me$_2$NH·BH$_3$ (**B**) and *i*Pr$_2$N═BH$_2$ (**A**) (eq 3).

RESULTS AND DISCUSSION

The inherent polarization of the B−N bond means that net transfer of hydrogen from an amine−borane to an aminoborane *formally* involves N-to-N transfer of a protic hydrogen and concomitant B-to-B transfer of a hydridic hydrogen. Although the overall transformation is simple, at least four general pathways can be envisaged (Scheme 2). The most direct pathway (**1**) involves simultaneous cleavage of N−H and B−H bonds in a concerted, bimolecular process, whereby both the hydridic and protic hydrogens are transferred in a single and thus rate-determining step. The second general class of pathways involves stepwise transfer, in which either N-to-N hydrogen transfer precedes B-to-B hydrogen transfer, or vice versa (**2** and **3**). For both pathways, covalent linear diborazane intermediates can be envisaged (**2a**, **3a**), or the reactions could involve stepwise radical (intermediates **2b**, **3b**) or ionic (intermediates **2c**, **3c**) hydrogen transfers or hydrogen transfers with accompanying B−N bond cleavage (intermediates **2d**, **3d**).

The final route we considered involves unimolecular dissociation of the amine−borane adduct **B**, leaving Me$_2$NH and BH$_3$ free in solution (**4**). Even at this stage, because BH$_3$·THF was not detected at any point in solution by ^{11}B NMR spectroscopy (δ_B = −1.1 ppm), formation of intermediates **2d** and **4** was considered unlikely. Moreover, the addition of BH$_3$ to *i*Pr$_2$N═BH$_2$ (**A**) connects intermediates **4** with **3d**, thus resulting in (unobserved) unproductive reactions, analogous to those occurring with the less substituted derivatives RNH$_2$·BH$_3$ (R = H, Me).[79] In order to more fully evaluate these mechanistic possibilities (Scheme 2), the kinetic and thermodynamic parameters of the hydrogen transfer, along with the influence of solvent and kinetic isotope effects, were determined by experimental and computational methods.

1. Experimental Data for Metal-Free Hydrogen Transfer from Me$_2$NH·BH$_3$ to *i*Pr$_2$N═BH$_2$. *1.1. Equilibrium between A + B and C + D.* We began by conducting an ^{11}B NMR spectroscopic study of the stoichiometric reaction of *i*Pr$_2$N═BH$_2$ (**A**, δ_B = 34.7 ppm, t, J_{BH} = 127 Hz) with Me$_2$NH·BH$_3$ (**B**, −13.9 ppm, q, J_{BH} = 97 Hz) at ambient temperature in THF (eq 3). Analysis by ^{11}B NMR spectroscopy, 18 h after mixing, revealed the signals arising from **A** and **B** to have decreased in intensity; concomitantly, two new species formed with signals at δ_B = −21.5 ppm (q, J_{BH} = 97 Hz)

dx.doi.org/10.1021/ja307247g | J. Am. Chem. Soc. 2012, 134, 16805−16816

Scheme 2. Initial Steps in General Pathways (1→4) for Hydrogen Transfer from $Me_2NH{\cdot}BH_3$ (B) to $iPr_2N{=}BH_2$ (A)

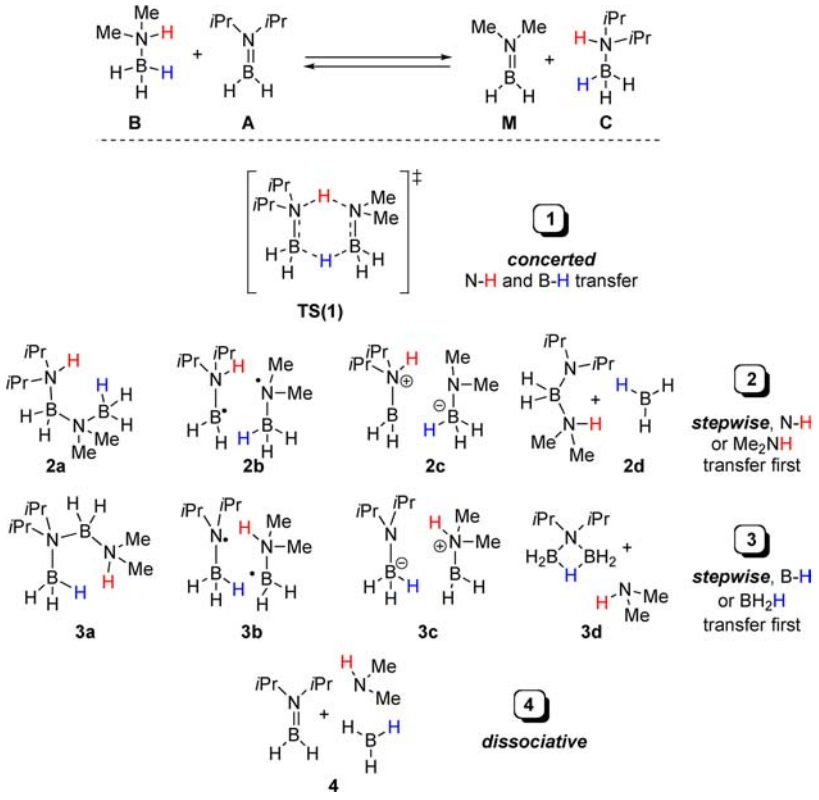

and 4.7 ppm (t, J_{BH} = 113 Hz), assigned to the known compounds $iPr_2NH{\cdot}BH_3$ (**C**) and $[Me_2N\text{-}BH_2]_2$ (**D**), respectively.[80,81] At this stage, 54% hydrogenation of **A** had occurred, and 58% of **B** had been dehydrogenated to cleanly furnish dimer **D**, as determined by integration of the peaks in the ^{11}B NMR spectrum. The monomeric precursor to **D**, aminoborane $Me_2N{=}BH_2$ (**M**), was not detected by ^{11}B NMR spectroscopy at this time, consistent with its known propensity for rapid dimerization in THF solution at 20 °C.[82,83] Allowing the reaction to stir for a further 20 days resulted in only a marginal increase in the relative intensities of the ^{11}B signals of **C** and **D**, indicating that the system had approached equilibrium. The hydrogen transfer process was then monitored by $^{11}B\{^1H\}$ NMR spectroscopy at 20 °C in THF solution (Figure 1), demonstrating that, within experimental error, equilibrium was established after 30 h (Figure 2a).

The same product mixture (**A**, **B**, **C**, **D**) was generated by a stoichiometric reaction of **C** (0.22 M) with **D** (0.11 M), which required 190 h at ambient temperature (Figure 2b). The attainment of a dynamic equilibrium was corroborated by reaction of **A** with $Me_2ND{\cdot}BD_3$ (d_4-**B**). After 2 h at 20 °C in THF solution, ^{11}B NMR spectroscopy indicated transfer of D_2, to predominantly generate $iPr_2ND{\cdot}BH_2D$ (d_2-**C**), as determined by the broad triplet characteristic of a BH_2D group (B−D coupling was not resolved, Figure 3b). As the reaction progressed, scrambling of deuterium into all of the B−H hydrogen environments was observed, as indicated by the disappearance of the distinct proton couplings in the ^{11}B NMR spectra.

1.2. Equilibrium Kinetics. Detailed $^{11}B\{^1H\}$ NMR spectroscopic analysis of the reaction of **A** (0.22 M) with **B** (0.22 M) at 22 °C in THF solution provided temporal−concentration data for all species, including the elusive monomeric aminoborane **M** (δ_B = 36.2 ppm, t, J_{BH} = 125 Hz), generated in low concentrations in the early stages of the reaction (Figure 4). A second data set was obtained using an excess of **B** (0.43 M, see Figure SI-1), and also the reverse approach to equilibrium (0.22 M **C** + 0.11 M **D**) was measured at 22 °C (see Figure SI-2). Analysis of the initial pseudo-first-order phase of the latter process (**C** + 0.5**D**) allowed direct extraction of the rate constant for monomerization of **D** (k_{-2}, Table 1) at 22 °C. Using this value, the kinetics for the forward reactions were then simulated (solid lines, Figure 4) according to a simple

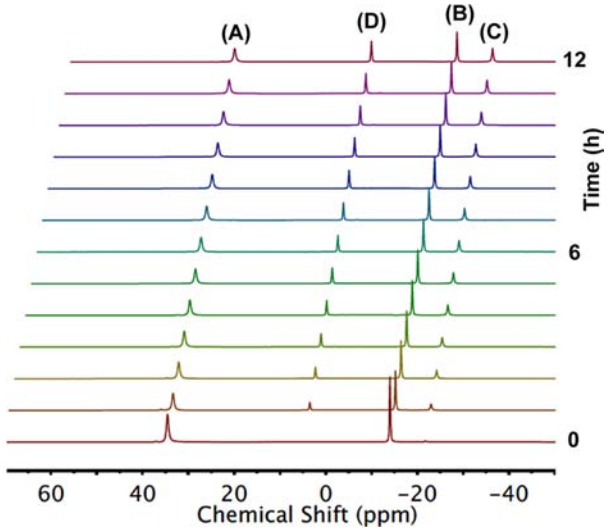

Figure 1. $^{11}B\{^1H\}$ NMR spectra of the reaction of $iPr_2N{=}BH_2$ (**A**) and $Me_2NH{\cdot}BH_3$ (**B**) (20 °C, THF, first 12 h) to generate $iPr_2NH{\cdot}BH_3$ (**C**) and $[Me_2N\text{-}BH_2]_2$ (**D**). Spectra are offset to the right to show individual peak intensities.

dx.doi.org/10.1021/ja307247g | J. Am. Chem. Soc. 2012, 134, 16805−16816

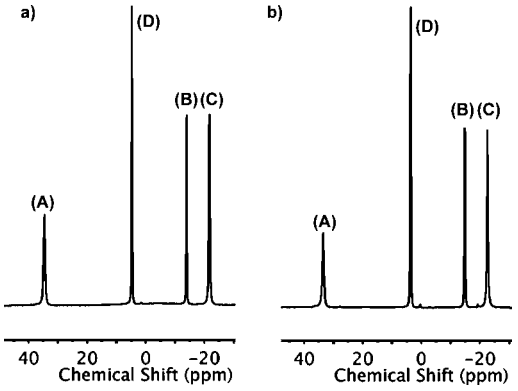

Figure 2. $^{11}B\{^1H\}$ NMR spectra (20 °C, THF) of the reactions of (a) iPr$_2$N=BH$_2$ (**A**) and Me$_2$NH·BH$_3$ (**B**) after 30 h, and (b) iPr$_2$NH·BH$_3$ (**C**) and [Me$_2$N-BH$_2$]$_2$ (**D**) after 190 h.

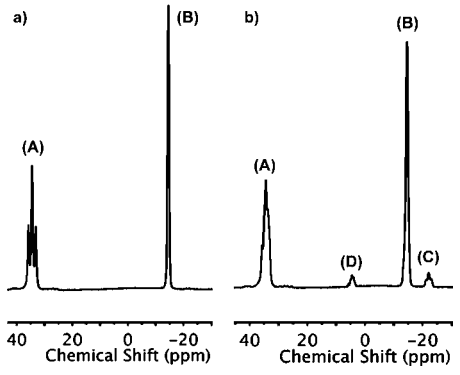

Figure 3. (a) ^{11}B NMR spectrum of iPr$_2$N=BH$_2$ (**A**) and Me$_2$ND·BD$_3$ (d_4-**B**) in THF at 20 °C. (b) The same system after 2 h, during which partial equilibration occurred to predominantly generate iPr$_2$ND·BH$_2$D (d_2-**C**) and [Me$_2$N-BD$_2$]$_2$ (d_4-**D**), plus isotopologues. On further reaction, complete redistribution of D/H occurs between all boron centers.

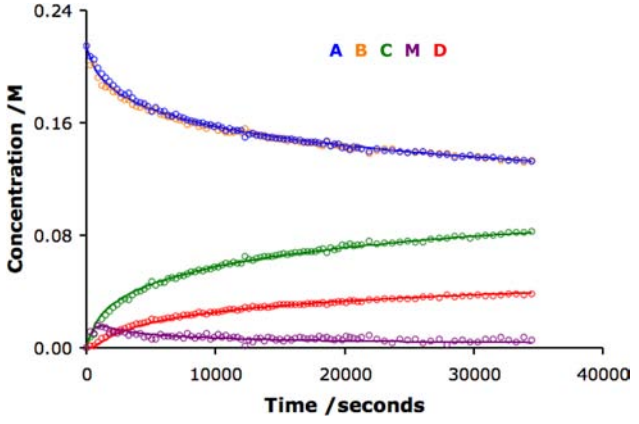

Figure 4. Reaction profile for the reaction of iPr$_2$N=BH$_2$ (**A**) with Me$_2$NH·BH$_3$ (**B**) (both 0.22 M, 22 °C, THF) to yield iPr$_2$NH·BH$_3$ (**C**) and Me$_2$N=BH$_2$ (**M**), and thus [Me$_2$N-BH$_2$]$_2$ (**D**) via dimerization (eq 5). Open circles are experimentally derived (^{11}B NMR) data; solid lines are simulations using the values for k_1, k_{-1}, k_2, and k_{-2} given in Table 1. Note the orange trace for B is obscured by that of A.

sequential equilibrium model (eq 5), thus yielding the remaining three rate constants (k_1, k_{-1} and k_2) and both equilibrium constants (Table 1, 22 °C). Consistent with the large value of K_2, kinetic simulations of the first 50% equilibration of **A** + **B** (ca. 3 × 10^4 s = 8.3 h) were found to be insensitive to k_{-2} (within experimental error) until k_{-2} was increased by 2 orders of magnitude.

Table 1. Rate and Equilibrium Constants Derived from Simulation of the Kinetics for Two-Stage Reaction (Eq 5) of iPr$_2$N=BH$_2$ (A) with Me$_2$NH·BH$_3$ (B) in THF

	temperature /°C				
	22	30	38	46	54
$k_1/10^{-4}$ M^{-1}·s^{-1}	5.1	9.1	11	16	18
error[a]/%	8.3	11	7.3	9.5	8.2
$k_{-1}/10^{-2}$ M^{-1}·s^{-1}	3.1	4.4	5.2	6.6	8.3
error[a]/%	10	13	8.6	11	10
$k_2/10^{-2}$ M^{-1}·s^{-1}	2.3	2.7	4.3	6.2	9.0
error[a]/%	4.1	4.8	3.5	4.3	4.2
k_{-2}[b]$/10^{-7}$ s^{-1}	2.3	8.1	27	82	240
k_{-1}/k_2	1.4	1.6	1.2	1.1	0.9
$K_1/10^{-2}$	1.7	2.0	2.1	2.4	2.2
$K_2/10^4$ M^{-1}	9.8	3.3	1.6	0.8	0.4

[a]Overall experimental deviation from the simulated model. [b]Values at 22 and 54 °C determined by analysis of kinetics of **C** + **D**; values at 30–46 °C are estimated; see text for discussion.

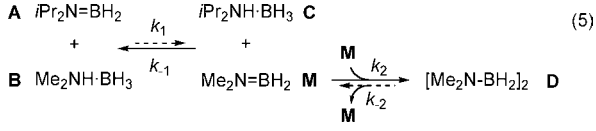

(5)

Simulations were then conducted with experimental data sets obtained for approach to equilibrium at 30, 38, 46, and 54 °C, from **A** (0.22 M) + **B** (0.22 and 0.43 M; see Figures SI-3–SI-10) as well as **C** (0.22 M) + **D** (0.11 M at 54 °C; see Figure SI-11). The model was again relatively insensitive to the magnitude of k_{-2} during the first 50% of equilibration,[84] with the simulations allowing extraction of k_1, k_{-1}, and k_2 (Table 1). The excellent correlations between simulation and experiment support the conclusion that the equilibrium (K_1) between **A** and **B** is driven forward by coupling to the sequential equilibrium (K_2) of **M** with 0.5**D**, as outlined in eq 5. The bimolecular rate constants for hydrogen transfer at 22 °C afford K_1 = (1.7 ± 0.3) × 10^{-2} (dimensionless). This endergonic equilibrium (K_1; ΔG_1° = +10 kJ·mol^{-1}) can be qualitatively understood to arise from the steric decompression arising on conversion from tetrahedral to trigonal planar geometry at nitrogen in the hydrogen donor. Essentially, therefore, the more hindered iPr$_2$NH·BH$_3$ (**C**) is a better hydrogen donor than Me$_2$NH·BH$_3$ (**B**), and conversely the less hindered Me$_2$N=BH$_2$ (**M**) is a more effective hydrogen acceptor than iPr$_2$N=BH$_2$ (**A**).

For the second step in the overall reaction (eq 5), the bimolecular rate constant k_2 = (2.3 ± 0.1) × 10^{-2} M^{-1}·s^{-1} (Table 1, 22 °C) compares well with the value of 1.0 × 10^{-2} M^{-1}·s^{-1} recently estimated by Weller and Lloyd-Jones for the dimerization of **M** generated during Rh-catalyzed dehydrocoupling of **B** in *o*-difluorobenzene.[85] In the current process (eq 5), the dimerization of **M** to generate [Me$_2$N-BH$_2$]$_2$ (**D**) is in

dx.doi.org/10.1021/ja307247g | J. Am. Chem. Soc. 2012, 134, 16805–16816

competition with capture by **C** in the reverse hydrogen transfer reaction (eq 6).

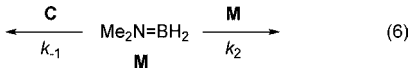

(6)

The bimolecular rate constants for these two processes are similar (k_{-1}/k_2 = 1.4 at 22 °C) and about 2 orders of magnitude greater than for the forward hydrogen transfer (k_1); moreover, until overall equilibrium (eq 5) is approached, the monomerization (k_{-2}) of **D** is orders of magnitude slower than any of the other processes. As a result, in the approach to equilibrium from **A** + **B**, the monomeric species **M** does not accumulate substantially; instead it reaches a relatively low maximum concentration ($[\mathbf{M}]_{max}$) early in the reaction. For the example in Figure 4, where $[\mathbf{A},\mathbf{B}]_o$ = 0.22 M, the relative rate of reverse hydrogen transfer over dimerization is approximately constant ($k_{-1}[\mathbf{C}]/k_2[\mathbf{M}]$ = 1.4) until ca. 1 × 10^3 s, after which it rises to the equilibrium value of ca. 232. This results in the maximum monomer concentration of 0.015 M being reached at ca. 1 × 10^3 s and then steadily decaying to reach $[\mathbf{M}_{eq}]$ = 0.0008 M. This propensity to undergo reverse hydrogen transfer (k_{-1}) results in the efficient redistribution of D and H at boron observed during the reaction of **A** and d_4-**B** (Figure 3).

1.3. Equilibrium Thermodynamics. The rate constants determined at five different temperatures (22, 30, 38, 46, and 54 °C, Table 1) were employed for Eyring analysis of the forward (k_1) and backward (k_{-1}) hydrogen transfers between *i*Pr_2N=BH_2 (**A**) and Me_2NH·BH_3 (**B**) (Figure SI-12). Linear regression of the data afforded $\Delta H^{\ddagger}$ and $\Delta S^{\ddagger}$ (Table 2) for both processes. Both hydrogen transfers involve large, negative entropies of activation (−201 to −210 J·mol^{-1}·K^{-1}), consistent with bimolecular assembly of a highly ordered activated complex, but rather low enthalpies (+21 to +29 kJ·mol^{-1}), suggesting that bond breaking accompanies bond making, i.e., that transfer is concerted. The free energies of activation (81−91 kJ·mol^{-1} at 295 K) are similar to those found for Diels−Alder reactions (∼100 kJ·mol^{-1}).[86]

By allowing samples of **A** + **B** (0.22 M in THF) to fully equilibrate, the apparent equilibrium constant (K_{eq}) for the *overall* process was determined by ^{11}B NMR spectroscopy, the equilibrium concentration of Me_2N=BH_2 (ca. 0.2% of total boron) being negligible. Using K_{eq} values determined at 25, 35, 45, 55, and 65 °C in THF, a Van't Hoff analysis was conducted (Table SI-1 and Figure SI-13). Linear regression afforded $\Delta H°$ and $\Delta S°$ (Table 3), with the reaction found to be slightly exergonic at 22 °C ($\Delta G°_{(295)}$ = −7 ± 2 kJ·mol^{-1}, Table 3; see also Table SI-2). The high entropic cost of dimerization of Me_2N=BH_2 (**M**) to generate $^1/_2[Me_2N\text{-}BH_2]_2$ (**D**) results in the overall reaction becoming endergonic above ca. 65 °C.

1.4. Effect of Solvent. To further probe the transition states involved in the overall reaction (eq 5), the influence of solvent on the rates of hydrogen transfer (k_1 and k_{-1}) and dimerization (k_2 and k_{-2}) was investigated. A range of polar, potentially coordinating solvents such as tetraglyme, acetonitrile, and dimethoxyethane were considered as well as polar, non-coordinating solvents such as dichloromethane and difluorobenzene and the relatively non-polar, non-coordinating solvent toluene. Kinetic data were acquired by ^{11}B{^{1}H} NMR spectroscopy and analyzed by simulation (Figures SI-14−SI-25) via the same procedures employed for the reaction in THF at 22 °C (see above), to afford the full complement of rate constants, and thus equilibrium constants, for each system (Table SI-3).

A key observation from these experiments is that there was only a small effect of the solvent on hydrogen transfer rates (k_1 ranged from (2.0−19) × 10^{-4} M^{-1}·s^{-1}, and k_{-1} from (5.6−23) × 10^{-2} M^{-1}·s^{-1}), with both rates being influenced similarly and thus rather small variations in K_1 ((1.1→14) × 10^{-3}). Overall these features suggest that there are only small changes in charge distribution between the reactants and the transition state, this strongly weighing against the formation of ionic intermediates such as **2c** and **3c**, and against polarized radical intermediates **2b** and **3b** (Scheme 2). In contrast, a more significant effect was found for the dimerization/monomerization equilibrium, with K_2 values ranging from (0.13→24) × 10^6 M^{-1}. Acetonitrile was found to substantially accelerate the dimerization (k_2 = 1.3 ± 0.3 M^{-1}·s^{-1}), consistent with recent reports on Rh-catalyzed dehydrocoupling of **B**, where **M** is an intermediate.[82,85]

1.5. Kinetic Isotope Effects for Hydrogen Transfer. As noted above, reversible hydrogen transfer between *i*Pr_2N=BH_2 (**A**) and Me_2ND·BD_3 (d_4-**B**) resulted in H/D redistribution at boron (Figure 3) in an overall process (eq 5) that proceeded more slowly than with **B** under the same conditions. To provide further information on the nature of the hydrogen transfer, temporal−concentration data were acquired (using ^{11}B{^{1}H} NMR spectroscopy) for four separate reactions at 22 °C, each employing different combinations of deuterium labeling in substrates **A** and **B**. Simulation of the kinetics (Figures 5 and SI-26−SI-29) according to the standard model (eq 5), employing k_{-2} derived from the unlabeled system, afforded k_1, k_{-1}, and k_2, and thus kinetic isotope effects (KIEs, k_H/k_D) associated with these steps (Table 4).

As expected, the net KIEs for dimerization (k_2) of **M**, where no B−D cleavage occurs, were small (average k_H/k_D = 1.1). However, the KIEs for hydrogen transfer were substantial in both directions (k_1 and k_{-1}), but only for the protic (N-to-N) transfer (average k_H/k_D = 6). In contrast, the hydridic (B-to-B) transfer was generally accompanied by a small inverse KIE (average k_H/k_D = 0.9), although it is not evident at this stage whether this arises from the hydrogen that is transferred or from the four spectating hydrogens on the two boron centers.

The large, normal KIE associated with deuterium transfer from nitrogen (Table 4) clearly indicates that N−H cleavage occurs in the rate-determining step. However, the small inverse

Table 2. Thermodynamic Activation Parameters[a] for Hydrogen Transfers between *i*Pr_2N=BH_2 (A) + Me_2NH·BH_3 (B) and *i*Pr_2NH·BH_3 (C) + Me_2N=BH_2 (M) at 22 °C

	A + B (k_1)		**C + M (k_{-1})**
$\Delta G_1^{\ddagger}{}_{(295)}$	91 ± 5 kJ·mol^{-1}	$\Delta G_{-1}^{\ddagger}{}_{(295)}$	81 ± 2 kJ·mol^{-1}
$\Delta S_1^{\ddagger}$ [b]	−210 ± 11 J·mol^{-1}·K^{-1}	$\Delta S_{-1}^{\ddagger}$ [b]	−201 ± 8 J·mol^{-1}·K^{-1}
$\Delta H_1^{\ddagger}$ [b]	29 ± 5 kJ·mol^{-1}	$\Delta H_{-1}^{\ddagger}$ [b]	21 ± 3 kJ·mol^{-1}

[a]From $\ln(k/T) = \Delta S^{\ddagger}/R + \ln(k_B/h) - \Delta H^{\ddagger}/RT$. [b]Linear regression of Figure SI-12; see Supporting Information.

dx.doi.org/10.1021/ja307247g | J. Am. Chem. Soc. 2012, 134, 16805−16816

Table 3. Thermodynamic Parameters Calculated for the *Overall* Reaction (Eq 3)

Van't Hoff analysis[a]		Eyring analysis[b]	
$\Delta G^\circ_{(295)}$[c]	-7 ± 2 kJ·mol^{-1}	$\Delta G^\circ_{(295)}$[c]	-18 ± 18 kJ·mol^{-1}
ΔS°[d]	-149 ± 20 J·mol^{-1}·K^{-1}	ΔS°	-187 ± 50 J·mol^{-1}·K^{-1}
ΔH°[d]	-51 ± 2 kJ·mol^{-1}	ΔH°	-73 ± 23 kJ·mol^{-1}

[a]From $\ln(K_{eq}) = \Delta S^\circ/R - \Delta H^\circ/RT$, where $K_{eq} = K_1^2K_2 = [\mathbf{C}_{eq}]^2[\mathbf{D}_{eq}]/[\mathbf{A}_{eq}]^2[\mathbf{B}_{eq}]^2$. [b]From data in Table 1, $\Delta X_n^\circ = \Delta X_n^\ddagger - \Delta X_{-n}^\ddagger$ and $\ln(k/T) = \Delta S^\ddagger/R + \ln(k_B/h) - \Delta H^\ddagger/RT$. [c]$\Delta G^\circ = \Delta H^\circ - T\Delta S^\circ$. [d]Linear regression of Figure SI-13.

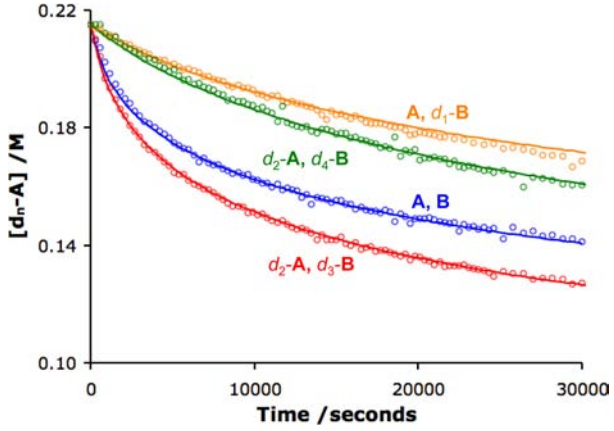

Figure 5. Experimental ($^{11}B\{^1H\}$ NMR, circles) and simulated (lines) temporal−concentration data for iPr$_2$N=B(H/D)$_2$ (d_n-**A**) in the reaction of d_n-**A** (0.22 M) with Me$_2$N(H/D)·B(H/D)$_3$ (d_n-**B**, 0.22 M), at 22 °C in THF.

Table 4. Rate Constants (Simulation, Figure 5) and KIEs (k_H/k_D) for Hydrogen Transfer (k_1 and k_{-1}) between iPr$_2$N=B(H/D)$_2$ (d_n-A) and Me$_2$N(H/D)·B(H/D)$_3$ (d_n-B) at 22 °C

reactants	k_1 /10^{-5} M^{-1}·s^{-1}	KIE (k_1) k_H/k_D	k_{-1} /10^{-3} M^{-1}·s^{-1}	KIE (k_{-1}) k_H/k_D
N=BH$_2$ (**A**) NH·BH$_3$ (**B**)	48 ± 3	–	32 ± 2	–
N=BH$_2$ (**A**) ND·BH$_3$ (d_1-**B**)	7.2 ± 0.5	6.7 ± 0.9	5.1 ± 1.2	6 ± 3
N=BD$_2$ (d_2-**A**) ND·BD$_3$ (d_4-**B**)	9.2 ± 0.7	5.2 ± 0.8	5.9 ± 1.2	5 ± 2
N=BD$_2$ (d_2-**A**) NHBD$_3$ (d_3-**B**)	55 ± 6	0.9 ± 0.2	23 ± 3	1.4 ± 0.3
N=BH$_2$ (**A**)[a] NH·BD$_3$ (d_3-**B**)	66 ± 7	0.7 ± 0.1	36 ± 4	0.9 ± 0.2

[a]Reaction proceeded with redistribution of deuterium and hydrogen at boron.

KIE associated with deuterium substitution on boron is consistent with B−H cleavage before, during (asynchronous), or after the rate-liming event, the latter requiring the inverse KIE to arise from the non-transferred hydrogens on boron. Thus, while study of the effect of solvent eliminated ionic intermediates **2b** and **3b** from consideration, and also weighed strongly against polarized intermediates **2c** and **3c**, a number of pathways, *inter alia* **1**, **2**, and **3** (via intermediates **2a** and **3a** respectively; Scheme 2) remained feasible, these being at least consistent with the KIEs.

In the latter two pathways, linear but isomeric diborazane (R$_2$NH-BH$_2$-NR′$_2$-BH$_3$) intermediates **2a** and **3a** would be generated. The absence of signals from these species in any of the ^{11}B NMR spectra would require them to be transient intermediates. However, preparation of a reference sample of linear diborazane iPr$_2$NH-BH$_2$-NMe$_2$-BH$_3$ demonstrated that this material is stable over a period of 24 h under the reaction conditions (see Supporting Information). With pathways **2**, **3**, and **4** largely dismissed via experiment, we turned to theoretical (DFT) calculations for further insight regarding the mechanism of hydrogen transfer.

2. DFT Calculations. *2.1. Pathway 1 versus 2, 3, and 4.* All of the pathways for reactions between iPr$_2$N=BH$_2$ (**A**) and Me$_2$NH·BH$_3$ (**B**) considered above were explored computationally by means of DFT calculations (Schemes 2 and 3, Table

Scheme 3. Selected Computed Species, Table 5

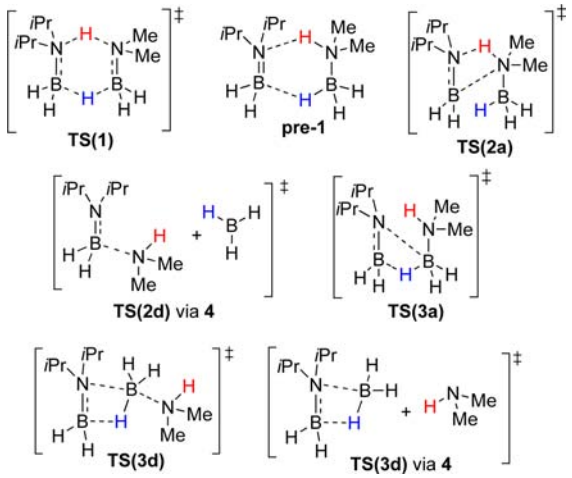

5, and Supporting Information). A common factor in the stepwise pathways (**2** and **3**, Scheme 2) is that the initial steps are endergonic. Indeed, the free energies of single hydrogen atom, proton, or hydride transfer pathways **2** and **3** (via intermediates **2b,c** and **3b,c**) are significantly higher than the free energy of activation for pathway **1**, via **TS(1)**. The same is true for other possible combinations of H$^{\bullet/+/-}$ transfer from boron or nitrogen of **B** to boron or nitrogen of **A**, respectively (see Supporting Information, Scheme SI-2 and Table SI-4).

Formation of the hydroamination intermediate **2a** (Scheme 2) may proceed via a very high barrier (**TS(2a)**, Scheme 3). The same is true for the formation of the hydroboration intermediate **3a** (Scheme 2) via **TS(3a)** (Scheme 3). By comparison, a related version of pathway **3**, which is associated with cleavage of the B−N bond of the amine−borane adduct **B** in the transition state **TS(3d)** (Scheme 3), has significantly lower free energy of activation.[87] However, the barrier is still higher than that of pathway **1**. Moreover, this reaction, affording the μ-amidodiborane H$_2$B(μ-H)(μ-NiPr$_2$)BH$_2$ and

dx.doi.org/10.1021/ja307247g | J. Am. Chem. Soc. 2012, 134, 16805−16816

Table 5. Computed Thermochemical Parameters for Reactions between *i*Pr$_2$N=BH$_2$ (A) and Me$_2$NH·BH$_3$ (B)[a]

reaction or TS	$\Delta G_{(295)}$ /kJ·mol^{-1}	$\Delta S_{(295)}$ /J·mol^{-1}·K^{-1}	$\Delta H_{(295)}$ /kJ·mol^{-1}
TS(1)[b]	+86.9	−190.8	+38.0
pathway **1**[b]	+9.1	−8.5	+13.9
pre-1[c,d]	–	–	–
TS(2a)[c]	+210.7	−189.1	+154.9
pathway **2** via **2a**[b]	+15.3	−202.4	−44.5
pathway **2** via **2b**[b]	+328.0	+54.6	+344.1
pathway **2** via **2c**[b,e]	+310.0	+5.1	+308.5
TS(2d) via **4**[c,f]	–	–	–
pathway **2** via **2d**[b]	+115.3	+1.3	+115.7
TS(3a)[c]	+252.9	−198.2	+194.4
pathway **3** via **3a**[b]	+63.6	−209.4	+1.8
pathway **3** via **3b**[b]	+326.1	+27.1	+334.1
pathway **3** via **3c**[b,e]	+336.8	+10.1	+339.8
TS(3d)[c]	+157.0	−161.3	+109.3
TS(3d) via **4**[c,f]	–	–	–
pathway **3** via **3d**[b]	+32.5	−22.9	+25.7
pathway **4**[b]	+108.9	+169.8	+159.0

[a]See pathways **1**–**4** in Scheme 2; see also Scheme 3. PBE0/6-31G(d,p), all values relative to separated reactants, **A** + **B**. [b]See Scheme 2. [c]See Scheme 3. [d]Not found. [e]In the cases of reactions that led to charge separation, the polar medium THF was mimicked by employing the implicit solvent model PCM (see Experimental Section). [f]Not located, presumably very flat barrier.

Me$_2$NH (intermediates **3d**, Scheme 2), is thermodynamically unfavored.[88]

The initial formation of solvent-separated Me$_2$NH and BH$_3$ via dissociation of the adduct **B** (intermediates **4**, Scheme 2) correlates with a significantly larger change in free energy compared to the formation of **TS(1)**. If dissociation of **B** occurred, Me$_2$NH or BH$_3$ could subsequently react with **A** to give the linear species *i*Pr$_2$N-BH$_2$-HNMe$_2$ (through **TS(2d)** via pathway **4**, Scheme 3) or H$_2$B(μ-H)(μ-N*i*Pr$_2$)BH$_2$ (through **TS(3d)** via pathway **4**, Scheme 3), respectively.[89] However, as both reactions and the preceding dissociation (to produce intermediates **4**, Scheme 2) are thermodynamically unfavorable, these pathways are presumably not in operation.

2.2. Concerted Hydrogen Transfer via TS(1). In contrast to all of the other pathways explored (**2**–**4**, see above), the computed activation parameters (22 °C) for hydrogen transfer from Me$_2$NH·BH$_3$ (**B**) to *i*Pr$_2$N=BH$_2$ (**A**) in a concerted fashion (via **TS(1)**) are in good agreement with the experimentally determined parameters ($\Delta G_1^{\ddagger}{}_{(295)}$ calc = 86.9 kJ·mol^{-1}, exp = 91 ± 5 kJ·mol^{-1}; $\Delta H_1^{\ddagger}{}_{(295)}$ calc = 38.0 kJ·mol^{-1}, exp = 29 ± 5 kJ·mol^{-1}; $\Delta S_1^{\ddagger}{}_{(295)}$ calc = −190.8 J·mol^{-1}·K^{-1}, exp = −210 ± 11 J·mol^{-1}·K^{-1}). The equilibrium transfer of hydrogen is predicted by the calculations to be endergonic by 9.1 kJ·mol^{-1}, consistent with the experimentally derived value ($\Delta G_1^{\circ}{}_{(295)}$ = 10 ± 7 kJ·mol^{-1}). Having found a pathway consistent with the experimental data, we tested, computationally, whether an intermediate complex is formed between **A** and **B** prior to concerted double hydrogen transfer. Using the computational method PBE0/6-31G(d,p), the complex **pre-1** (Scheme 3) was not found.[90]

Concerted hydrogen transfer was investigated in more detail using three different density functionals, each in combination with basis sets of double- and triple-ζ quality. The structure of the six-membered transition state, **TS(1)**, calculated with the hybrid functional PBE0 and the 6-31G(d,p) basis, is shown in Figure 6.[91]

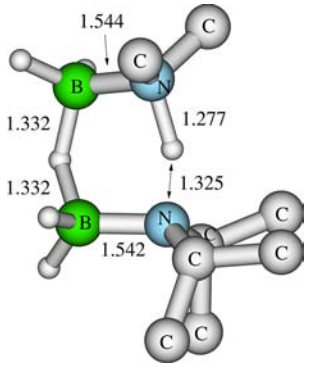

Figure 6. PBE0/6-31G(d,p)-calculated structure of the transition state **TS(1)** for concerted hydrogen transfer from Me$_2$NH·BH$_3$ (**B**) to *i*Pr$_2$N=BH$_2$ (**A**). C-bonded hydrogen atoms omitted for clarity; distances in Å.

2.3. Theoretical versus Experimental KIEs. As noted above, the experimental KIEs for hydrogen transfer were substantial, but only for the protic (N-to-N) transfer (k_H/k_D = 6.7 ± 0.9), with deuteration at boron inducing a small inverse KIE (k_H/k_D = 0.9 ± 0.2). In order to reconcile this phenomenon with a concerted process, hydrogen transfer must be asynchronous, with the B-to-B transfer of the hydridic hydrogen being substantially advanced over the N-to-N transfer of the protic hydrogen at the transition state. The KIEs associated with deuteration at nitrogen and/or boron were calculated by means of conventional transition state theory, combined with Wigner's tunneling correction[92] (Tables 6 and SI-5).

Table 6. Theoretical versus Experimental Deuterium KIEs for Hydrogen Transfer from Me$_2$N(H/D)·B(H/D)$_3$ to *i*Pr$_2$N=B(H/D)$_2$[a]

	KIE, k_H/k_D (k_1)	
transfer (**B** to **A**)	calculated	experimental[b]
ND·BH$_3$ to N=BH$_2$	6.3	6.7 ± 0.9
ND·BD$_3$ to N=BD$_2$	4.9	5.2 ± 0.8
NH·BD$_3$ to N=BD$_2$	0.8	0.9 ± 0.2
NH·BH$_2$*D* to N=BH$_2$	1.0	–
NH·BD$_2$*H* to N=BD$_2$	0.8	–

[a]Theoretical values calculated via **TS(1)** (PBE0/6-31G(d,p)), including Wigner's tunneling correction. [b]Data from Table 4.

Deuteration at nitrogen gave a large normal KIE, while deuteration at boron gave a small and inverse KIE. Altogether, the calculated values are in good agreement with the experimental values, supporting the conclusion that hydrogen transfer proceeds via an asynchronous concerted transition state **TS(1)**.

In order to better understand the KIEs arising from deuteration at boron, two further reactions involving *selectively* deuterated species were calculated, reactions which were presently not feasible to investigate experimentally: (i) an H−D selective hydrogen transfer reaction from Me$_2$NH·BH$_2$D (d_1-**B**) to *i*Pr$_2$N=BH$_2$ (**A**), and (ii) an H−H selective hydrogen transfer reaction from Me$_2$NH·BD$_2$H (d_2-**B**) to *i*Pr$_2$N=BD$_2$ (d_2-**A**). For case (i), it was calculated that there was no KIE present, while for case (ii), a small, inverse KIE was

dx.doi.org/10.1021/ja307247g | J. Am. Chem. Soc. 2012, 134, 16805−16816

obtained. Thus, the net KIEs observed experimentally for deuteration on boron arise predominantly from inverse secondary KIEs related to changes in geometry at both boron centers during the hydrogen transfer process; the primary KIE for the hydridic transfer is small and normal.

2.4. Dimerization of $Me_2N{=}BH_2$ (M). The dimerization of the aminoborane $Me_2N{=}BH_2$ (**M**) to give $[Me_2N\text{-}BH_2]_2$ (**D**) proceeds via a concerted pathway. This [2+2] cycloaddition has been treated computationally on different occasions before, whereas the thermochemical character of the reaction has been calculated with different methods to be either endergonic[82,93] or exergonic[44,82] at ambient conditions. Using PBE0/6-31G(d,p), we found the reaction to be exergonic by −20.0 kJ·mol^{-1} at 22 °C, consistent with the experimentally determined value ($\Delta G_2^{\circ}{}_{(295)}$ = −28 ± 14 kJ·mol^{-1}, see Table SI-2). The computed thermochemical reaction and activation parameters (Table 7) were also in good agreement with the experimentally determined values ($\Delta G_2^{\ddagger}{}_{(295)}$ calc = 89.6 kJ·mol^{-1}, exp = 82 ± 8 kJ·mol^{-1}; $\Delta H_2^{\ddagger}{}_{(295)}$ calc = 37.2 kJ·mol^{-1}, exp = 33 ± 9 kJ·mol^{-1}; $\Delta S_2^{\ddagger}{}_{(295)}$ calc = −177.5 J·mol^{-1}·K^{-1}, exp = −164 ± 30 J·mol^{-1}·K^{-1}; see Table SI-2 and Figure SI-33 for the calculated structure of the transition state).

Table 7. Computed Thermochemical Parameters for the Dimerization of $Me_2N{=}BH_2$ (M) To Give $[Me_2N\text{-}BH_2]_2$ (D) (PBE0/6-31G(d,p))

reaction or TS	$\Delta G_{(295)}$ /kJ·mol^{-1}	$\Delta S_{(295)}$ /J·mol^{-1}·K^{-1}	$\Delta H_{(295)}$ /kJ·mol^{-1}
TS (2M→D)	+89.6	−177.5	+37.2
reaction (2M→D)	−20.0	−200.0	−79.0

3. Overall Energetic Landscape and Comparison with Other Systems. The above experimental analyses of the hydrogen transfer and dimerization equilibria, supported by computational (DFT) studies, provide the kinetic and thermodynamic information (Tables 2, 3, and SI-2) required to construct a full energetic landscape for the system (Scheme 4). Transfer occurs via an asynchronous concerted pathway (**1**, Scheme 2), with the B-to-B hydridic transfer advanced over the N-to-N protic transfer at the transition state; these timings are reflected in small and large primary KIEs, respectively. Eyring analysis indicates that, at ambient temperature, the hydrogen transfer reaction is slightly endergonic in the forward direction ($\Delta G_1^{\circ}{}_{(295)}$ = 10 ± 7 kJ·mol^{-1}), and the dimerization of $Me_2N{=}BH_2$ is exergonic ($\Delta G_2^{\circ}{}_{(295)}$ = −28 ± 14 kJ·mol^{-1}), predicting the overall reaction to be exergonic ($\Delta G^{\circ}{}_{(295)}$ = −18 ± 18 kJ·mol^{-1}), in good agreement with the value determined by Van't Hoff analysis ($\Delta G^{\circ}{}_{(295)}$ = −7 ± 2 kJ·mol^{-1}). It is the coupling of the hydrogen transfer to the slow but exergonic dimerization of **M** that, at the concentrations employed (ca. 0.2−0.4 M), drives the process substantially forward (toward **C** and **D**) at ambient temperature.

It is instructive to compare the hydrogen transfer reaction (Scheme 4) to the $NH_3{\cdot}BH_3$-mediated reductions of imines and polar alkenes. Detailed studies by Berke,[43,51,75,76,94−97] including isotopic labeling to determine KIEs and theoretical calculations, have shown these two reactions to be mechanistically distinct, depending on the hydrogen acceptor involved (Scheme 5).[51,75,97]

Scheme 5. Berke's Mechanisms for Hydrogen Transfer to (i) Imines and (ii) Polar Olefins

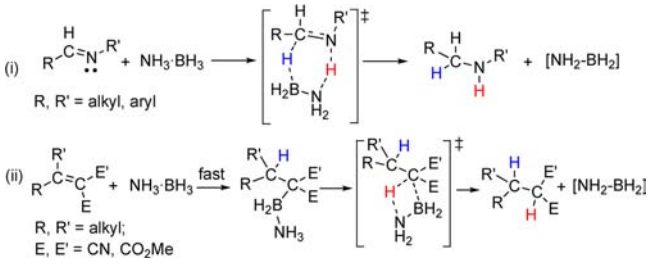

Scheme 4. Energetic Landscape for Overall Hydrogen Transfer Reaction: $i\text{Pr}_2N{=}BH_2$ (A) + $Me_2NH{\cdot}BH_3$ (B)

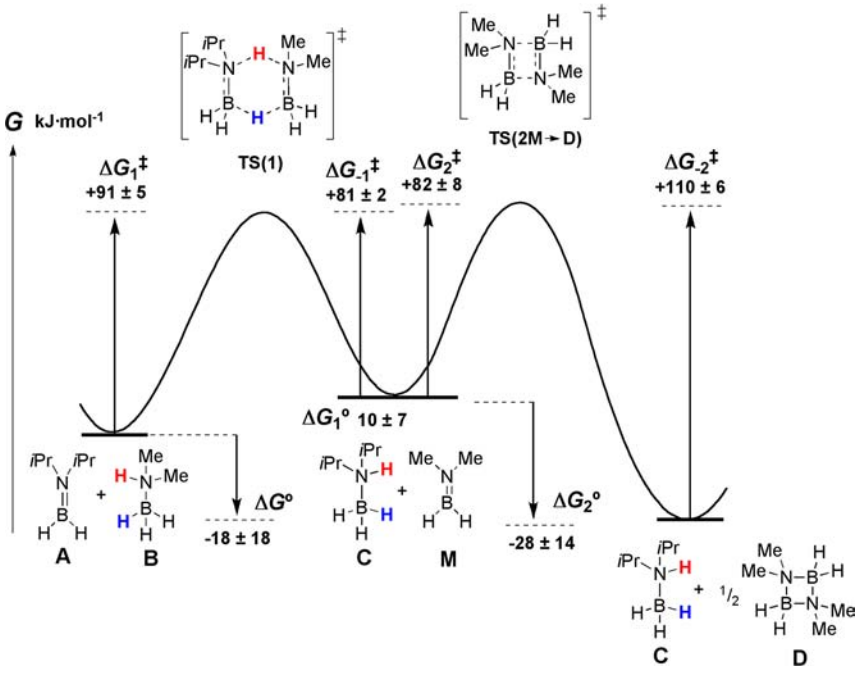

dx.doi.org/10.1021/ja307247g | J. Am. Chem. Soc. 2012, 134, 16805−16816

The hydrogenation of imines ((i), Scheme 5) is postulated to occur via a concerted transition state. The experimental KIEs for this transformation (R = R′ = Ph) are small for both the B-to-C transfer (k_H/k_D = 0.87, using $NH_3{\cdot}BD_3$) and the N-to-N transfer (k_H/k_D = 1.93, using $ND_3{\cdot}BH_3$), with $ND_3{\cdot}BD_3$ giving k_H/k_D = 1.39.[51] The imine hydrogenation is strongly exergonic (DFT calculated $\Delta G^\circ = -92$ kJ·mol^{-1}), thus predicting an early transition state for concerted transfer and leading to strongly attenuated primary KIEs. The inverse values for the B-to-C hydrogen transfer may arise through a secondary KIE from the BD_2 unit, rather than through the hydrogen transfer itself, analogous to our findings with **A** + **B** (Table 6).

The mechanism for hydrogenation of polar olefins is postulated to involve a fast hydroboration step prior to transfer of the protic hydrogen on nitrogen in a concerted transition state ((ii), Scheme 5). This mechanism was proposed on the basis of the detection of the hydroboration intermediate, as well as a primary KIE (k_H/k_D = 1.55) attending the N-to-C transfer of hydrogen.[75]

It is thus apparent that the mechanism of hydrogen transfer to iPr$_2$N═BH$_2$ is more similar in character to the reaction of $NH_3{\cdot}BH_3$ with imines (i) than polar olefins (ii), which is in line with measured electronegativities.[98] However, hydrogen transfer to iPr$_2$N═BH$_2$ is much less energetically biased ($\Delta G_1^\circ{}_{(295)}$ = 10 ± 7 kJ·mol^{-1}) than the reaction with imines. As a result, the much more symmetrical and linear N-to-N transfer of the protic hydrogen leads to the substantially greater KIE (k_H/k_D = 6.7) observed with transfer to iPr$_2$N═BH$_2$.[99,100]

CONCLUSIONS

Our in-depth studies have shown that the transfer of hydrogen from $Me_2NH{\cdot}BH_3$ (**B**) to iPr$_2$N═BH$_2$ (**A**) occurs directly, in a bimolecular, concerted, asynchronous, single-step process involving a six-membered transition state (**TS(1)**, Figure 6, Scheme 4). This is reminiscent of the mechanism postulated for the reduction of imines by $NH_3{\cdot}BH_3$ (Scheme 5). It is, however, endergonic, and the net conversion of **A** and **B** into 62% iPr$_2$NH·BH$_3$ (**C**) and [Me$_2$N-BH$_2$]$_2$ (**D**) via their stoichiometric equilibration (0.22 M) at 22 °C is driven by the exergonic dimerization of the transient Me$_2$N═BH$_2$ (**M**) produced. At 22 °C, the *overall* equilibrium is slightly exergonic ($\Delta G^\circ_{(295)} = -18 \pm 18$ kJ·mol^{-1}), with the hydrogen transfer ($\Delta G_1^\circ{}_{(295)}$ = 10 ± 7 kJ·mol^{-1}) only just outweighed by the dimerization of Me$_2$N═BH$_2$ ($\Delta G_2^\circ{}_{(295)} = -28 \pm 14$ kJ·mol^{-1}); the process becomes endergonic above 65 °C. The free energy necessary to traverse from iPr$_2$N═BH$_2$ (**A**) and $Me_2NH{\cdot}BH_3$ (**B**) to the transition state is $\Delta G_1^{\ddagger}{}_{(295)} = 91 \pm 5$ kJ·mol^{-1}, with enthalpic and entropic changes similar to a Diels–Alder reaction. The kinetic and thermodynamic parameters, including KIEs, experimentally determined for hydrogen transfer from $Me_2NH{\cdot}BH_3$ to iPr$_2$N═BH$_2$ are in good agreement with DFT calculations.

Our ongoing research in this area includes the determination of the steric and electronic effects associated with transfer of hydrogen, expanding the scope of the reaction, and the determination of whether the mechanistic model presented herein can be generalized for all amine–borane to aminoborane hydrogen transfer reactions. We are also currently exploring the utility of this interesting and unexpected chemistry in the formation of polymeric materials and the rehydrogenation of other multiply bonded acyclic and cyclic boron–nitrogen species.

EXPERIMENTAL SECTION

General Procedures, Reagents, and Equipment. All manipulations were carried out under an atmosphere of nitrogen gas using standard vacuum line and Schlenk techniques, or under an atmosphere of argon within an MBraun glovebox. All solvents were dried via a Grubbs design solvent purification system.[101] Deuterated solvents were purchased from Sigma Aldrich Ltd. and distilled from CaH_2 prior to use. $Me_2NH{\cdot}BH_3$, trimethylsilyl chloride (TMS-Cl), iPr$_2$NH, B(H/D)$_3$·THF, and B(OiPr)$_3$ were purchased from Sigma Aldrich Ltd. and purified by sublimation or distillation prior to use. nBuLi (1.6 M in hexane) was also purchased from Sigma Aldrich Ltd., and was used without further purification. $Me_2NH{\cdot}BD_3$, $Me_2ND{\cdot}BH_3$, and $Me_2ND{\cdot}BD_3$ were synthesized according to literature procedures,[83] and were all sublimed prior to use. iPr$_2$N═BH$_2$, [Me$_2$N-BH$_2$]$_2$ and iPr$_2$NH·BH$_3$ were synthesized via literature methods[40,80] and purified by distillation or sublimation prior to use.

NMR spectra were recorded using JEOL JNM-ECP300 or JNM-LA300 spectrometers. Chemical shifts are reported relative to external standards: $BF_3{\cdot}OEt_2$ (^{11}B). Integration of ^{11}B NMR spectra was performed using ACD Laboratories Version 9.13 or MestReNova Version 7.1.1-9649, with an estimated accuracy of ±5%. Calibration tests were performed to determine that the tri- and tetra-coordinate boron environments have similar relaxation times to ensure that the integrations were accurate and could be compared throughout. Kinetic and thermodynamic experiments, where peaks were monitored over time, were performed in the presence of an internal standard of B(OiPr)$_3$, neat, in a sealed capillary tube for increased accuracy. Kinetics were simulated by automated iteration of temporal–concentration data for all reliable species (generally **A**, **B**, **C**, **D**, and **M**—although when ^{11}B NMR spectral overlap occurred, selected species were employed) using Dynochem software (Scale-up Systems Ltd., Dublin, Eire) until satisfactory fits were obtained within the range of rate constants and errors reported in Tables 1 and 4, and in the Supporting Information.

Reaction of iPr$_2$N═BH$_2$ (A) with $Me_2NH{\cdot}BH_3$ (B). A 0.83 M solution of iPr$_2$N═BH$_2$ (**A**, 1.00 mL, 0.83 mmol) in THF was added to solid $Me_2NH{\cdot}BH_3$ (**B**, 49 mg, 0.83 mmol) and the mixture was then stirred over 18 h at 20 °C before analysis by ^{11}B NMR spectroscopy. ^{11}B NMR (96 MHz, THF): 34.7 (t, J_{BH} = 127 Hz, iPr$_2$N═BH$_2$), 4.7 (t, J_{BH} = 113 Hz, [Me$_2$N-BH$_2$]$_2$), −13.9 (q, J_{BH} = 97 Hz, $Me_2NH{\cdot}BH_3$), −21.5 (q, J_{BH} = 97 Hz, iPr$_2$NH·BH$_3$). At this point, analysis of the peak integrals in the ^{11}B NMR spectrum indicated 54% conversion of iPr$_2$N═BH$_2$ to iPr$_2$NH·BH$_3$ (**C**) and 58% conversion of $Me_2NH{\cdot}BH_3$ to [Me$_2$N-BH$_2$]$_2$ (**D**).

The reaction was then allowed to stir for an additional 30 h at 20 °C before further analysis by ^{11}B NMR spectroscopy, which indicated a change in the product distributions, but no change in the products themselves. After this time period, conversion of iPr$_2$N═BH$_2$ (**A**) to iPr$_2$NH·BH$_3$ (**C**), reached 58% and conversion of $Me_2NH{\cdot}BH_3$ (**B**) to [Me$_2$N-BH$_2$]$_2$ (**D**), 62%.

Reaction of [Me$_2$N-BH$_2$]$_2$ (D) with iPr$_2$NH·BH$_3$ (C). A solution of iPr$_2$NH·BH$_3$ (**C**, 91 mg, 0.79 mmol) in THF (2 mL) was added to solid [Me$_2$N-BH$_2$]$_2$ (**D**, 45 mg, 0.40 mmol). The mixture was then stirred over 18 h at 20 °C before analysis by ^{11}B NMR spectroscopy. ^{11}B NMR (96 MHz, THF): 34.7 (t, J_{BH} = 127 Hz, iPr$_2$N═BH$_2$), 4.7 (t, J_{BH} = 113 Hz, [Me$_2$N-BH$_2$]$_2$), −13.9 (q, J_{BH} = 97 Hz, $Me_2NH{\cdot}BH_3$), −21.5 (q, J_{BH} = 97 Hz, iPr$_2$NH·BH$_3$). At this point, analysis of the peak integrals indicated 6% conversion of iPr$_2$NH·BH$_3$ to iPr$_2$N═BH$_2$ and 7% conversion of [Me$_2$N-BH$_2$]$_2$ to $Me_2NH{\cdot}BH_3$. The reaction was then allowed to stir for an additional 172 h at 20 °C before further analysis by ^{11}B NMR spectroscopy, which indicated a change in the product distributions, but no change in the products themselves. After this time period, 35% conversion of iPr$_2$NH·BH$_3$ to iPr$_2$N═BH$_2$ and 38% conversion of [Me$_2$N-BH$_2$]$_2$ to $Me_2NH{\cdot}BH_3$ was observed.

General Reaction Conditions for Kinetic and Thermodynamic Measurements of $Me_2NH{\cdot}BH_3$ with iPr$_2$N═BH$_2$. A 0.22 M solution of iPr$_2$N═BH$_2$ (**A**, 2.0 mL, 0.43 mmol) was added to solid $Me_2NH{\cdot}BH_3$ (**B**, 25 mg, 0.43 mmol). An aliquot of this mixture (0.7

mL) was removed to a J-Young NMR tube containing an internal standard ($B(OiPr)_3$), and the reaction progress was monitored over time using $^{11}B\{^1H\}$ NMR spectroscopy at a minimum of 3 min intervals at a set temperature. The data obtained from these reactions was simulated to derived rate constants k_1, k_{-1}, k_2, with k_{-2} pre-established or estimated.[84] For equilibrium studies, the tube was heated for 3−4 days at the chosen temperature and then monitored at the temperature for 12 h without change to determine equilibrium position.

Synthesis of $iPr_2NH{\cdot}BD_3$. Freshly distilled $BD_3{\cdot}THF$ (25 mL, 25 mmol) was cooled to −78 °C and iPr_2NH was added dropwise to the borane. The solution was stirred at −78 °C for 15 min before warming to 22 °C for a further hour of reaction time. Volatiles were removed to yield the product as a clear, colorless oil (0.99 g, 8.4 mmol, 34%). ^{11}B NMR (96 MHz, $CDCl_3$): −22.6 (s).[80]

Synthesis of $iPr_2N{=}BD_2$. At −78 °C, 1.6 M *n*BuLi (5.2 mL, 8.4 mmol) was added dropwise to a solution of $iPr_2NH{\cdot}BD_3$ (0.99 g, 8.4 mmol) in THF (20 mL). The solution was stirred at −78 °C for 15 min before warming to 20 °C for a further hour of reaction time. At −78 °C, TMS-Cl (1.1 mL, 8.4 mmol) was added via syringe to the reaction mixture. The solution was stirred at −78 °C for 15 min prior to warming to 20 °C and stirring for 1 h further. To remove the LiCl byproduct, the solution was vacuum transferred. The product was left as a 0.22 M solution in THF for further use. ^{11}B NMR (96 MHz, THF): 34.1 (br s).[80]

Qualitative Test for Scrambling with $iPr_2N{=}BH_2$ and $Me_2ND{\cdot}BD_3$. To gain further mechanistic information, the reaction of $iPr_2N{=}BH_2$ (**A**) with $Me_2ND{\cdot}BD_3$ (d_4-**B**) was monitored by ^{11}B NMR spectroscopy. Strong evidence of an initial transfer of D_2 to $iPr_2N{=}BH_2$ (**A**) to form $iPr_2ND{\cdot}BH_2D$ (d_2-**C**), present as a broadened triplet at −21.0 ppm in the ^{11}B NMR spectrum, was observed. After 18 h, 37% conversion of $iPr_2N{=}BH_2$ (**A**) to $iPr_2ND{\cdot}B(H/D)_3$ (d_n-**C**) was determined, along with 32% conversion of $Me_2ND{\cdot}BD_3$ (d_4-**B**) to $[Me_2N\text{-}B(D/H)_2]_2$ (d_n-**D**). Scrambling of hydrogen and deuterium into all components of the reaction mixture was also apparent by ^{11}B NMR spectroscopy, with the sharp triplet initially corresponding to $iPr_2N{=}BH_2$ rapidly being broadened into a poorly defined multiplet.

General Reaction Conditions for Kinetic Measurements of Transferring HD and D_2 against H_2 To Determine KIEs. A 0.22 M solution of $iPr_2N{=}B(H/D)_2$ (d_n-**A**, 2.0 mL, 0.43 mmol) in THF was added to solid $Me_2N(H/D){\cdot}B(H/D)_3$ (d_n-**B**, 25−26 mg, 0.43 mmol). An aliquot of this mixture (0.7 mL) was removed to a J-Young NMR tube containing an internal standard ($B(OiPr)_3$), and the reaction progress was monitored over time using $^{11}B\{^1H\}$ NMR spectroscopy at a minimum of 5 min intervals. The data obtained from these reactions were simulated using Dynochem and rate constants were determined.

Computational Methods. DFT calculations were carried out with the Gaussian 09 program package.[102] Optimizations were performed with the exchange-correlation hybrid functional PBE0 of Adamo and Barone,[103] based on the pure functional of Perdew, Burke, and Ernzerhof[104,105] in combination with the valence-double-ζ basis set 6-31G(d,p).[106−111] For transition states, excellent initial guesses were obtained through relaxed surface scans along the major reaction coordinates. All stationary points were characterized as minima or transition states, respectively, by analytical vibrational frequency calculations. KIEs were calculated by means of conventional transition state theory including Wigner's tunneling correction.[92] In the cases of reactions that led to charge separation, the polar environment was taken into account by single-point calculations on the obtained geometries using the same density functional−basis set combination as specified above and including the implicit solvent model PCM (Polarizable Continuum Model) in the integral equation formalism variant (IEFPCM) with parameters for THF.[112−123] Zero-point corrections and thermal corrections to free energies were adopted from frequencies calculations on the level of optimization.

■ ASSOCIATED CONTENT

Ⓢ Supporting Information

All experimental reaction profiles of monitored kinetic data with overlaid simulated data, equilibrium data, and details of the DFT studies. This material is available free of charge via the Internet at http://pubs.acs.org.

■ AUTHOR INFORMATION

Corresponding Author

guy.lloyd-jones@bris.ac.uk; ian.manners@bris.ac.uk

Present Address

[†]Institute of Inorganic Chemistry, RWTH Aachen University, Landoltweg 1, 52056 Aachen, Germany

Notes

The authors declare no competing financial interest.

■ ACKNOWLEDGMENTS

E.M.L., N.E.S., A.P.M.R., and I.M. acknowledge the EPSRC for funding. E.M.L. is grateful to the EU for a Marie Curie postdoctoral fellowship. H.H. thanks the Deutsche Forschungsgemeinschaft (DFG) for a postdoctoral research fellowship. G.C.L.-J. is a Royal Society Wolfson Research Merit Award Holder. We thank Prof. Dr. Jeremy Harvey for useful discussions.

■ REFERENCES

(1) Staubitz, A.; Robertson, A. P. M.; Manners, I. *Chem. Rev.* **2010**, *110*, 4079.
(2) Staubitz, A.; Robertson, A. P. M.; Sloan, M. E.; Manners, I. *Chem. Rev.* **2010**, *110*, 4023.
(3) Campbell, P. G.; Marwitz, A. J. V.; Liu, S.-Y. *Angew. Chem., Int. Ed.* **2012**, *51*, 6074.
(4) Paetzold, P. *Adv. Inorg. Chem.* **1987**, *31*, 123.
(5) Zeng, H.; Zhi, C.; Zhang, Z.; Wei, X.; Wang, X.; Guo, W.; Bando, Y.; Golberg, D. *Nano Lett.* **2010**, *10*, 5049.
(6) Gutowska, A.; Li, L. Y.; Shin, Y. S.; Wang, C. M. M.; Li, X. H. S.; Linehan, J. C.; Smith, R. S.; Kay, B. D.; Schmid, B.; Shaw, W.; Gutowski, M.; Autrey, T. *Angew. Chem., Int. Ed.* **2005**, *44*, 3578.
(7) Whittell, G. R.; Manners, I. *Angew. Chem., Int. Ed.* **2011**, *50*, 10288.
(8) Chen, X.; Zhao, J.-C.; Shore, S. G. *J. Am. Chem. Soc.* **2010**, *132*, 10658.
(9) Hutchins, R. O.; Learn, K.; Nazer, B.; Pytlewski, D.; Pelter, A. *Org. Prep. Proced. Int.* **1984**, *16*, 335.
(10) Hamilton, C. W.; Baker, R. T.; Staubitz, A.; Manners, I. *Chem. Soc. Rev.* **2009**, *38*, 279.
(11) Stephens, F. H.; Pons, V.; Baker, R. T. *Dalton Trans.* **2007**, 2613.
(12) Dresselhaus, M. S.; Thomas, I. L. *Nature* **2001**, *414*, 332.
(13) Cho, A. *Science* **2004**, *303*, 942.
(14) Satyapal, S.; Petrovic, J.; Read, C.; Thomas, G.; Ordaz, G. *Catal. Today* **2007**, *120*, 246.
(15) Satyapal, S.; Petrovic, J.; Thomas, G. *Sci. Am.* **2007**, *296*, 80.
(16) Schlapbach, L. *Nature* **2009**, *460*, 809.
(17) Schlapbach, L.; Züttel, A. *Nature* **2001**, *414*, 353.
(18) Sutton, A. D.; Burrell, A. K.; Dixon, D. A.; Garner, E. B.; Gordon, J. C.; Nakagawa, T.; Ott, K. C.; Robinson, J. P.; Vasiliu, M. *Science* **2011**, *331*, 1426.
(19) Hausdorf, S.; Baitalow, F.; Wolf, G.; Mertens, F. O. R. L. *Int. J. Hydrogen Energy* **2008**, *33*, 608.
(20) For a multistep hydrogenation of a BN species, see: Luo, W.; Campbell, P. G.; Zakharov, L. N.; Liu, S.-Y. *J. Am. Chem. Soc.* **2011**, *133*, 19326.
(21) Staubitz, A.; Presa Soto, A.; Manners, I. *Angew. Chem., Int. Ed.* **2008**, *47*, 6212.

(22) Liu, Z.; Song, L.; Zhao, S.; Huang, J.; Ma, L.; Zhang, J.; Lou, J.; Ajayan, P. M. *Nano Lett.* **2011**, *11*, 2032.
(23) Dallanegra, R.; Robertson, A. P. M.; Chaplin, A. B.; Manners, I.; Weller, A. S. *Chem. Commun.* **2011**, *47*, 3763.
(24) Ewing, W. C.; Marchione, A.; Himmelberger, D. W.; Carroll, P. J.; Sneddon, L. G. *J. Am. Chem. Soc.* **2011**, *133*, 17093.
(25) Dietrich, B. L.; Goldberg, K. I.; Heinekey, D. M.; Autrey, T.; Linehan, J. C. *Inorg. Chem.* **2008**, *47*, 8583.
(26) Johnson, H. C.; Robertson, A. P. M.; Chaplin, A. B.; Sewell, L. J.; Thompson, A. L.; Haddow, M. F.; Manners, I.; Weller, A. S. *J. Am. Chem. Soc.* **2011**, *133*, 11076.
(27) Dallanegra, R.; Chaplin, A. B.; Tsim, J.; Weller, A. S. *Chem. Commun.* **2010**, *46*, 3092.
(28) (a) Alcaraz, G.; Sabo-Etienne, S. *Angew. Chem., Int. Ed.* **2010**, *49*, 7170. (b) Alcaraz, G.; Vendier, L.; Clot, E.; Sabo-Etienne, S. *Angew. Chem., Int. Ed.* **2010**, *49*, 918.
(29) Forster, T. D.; Tuononen, H. M.; Parvez, M.; Roesler, R. *J. Am. Chem. Soc.* **2009**, *131*, 6689.
(30) (a) O'Neill, M.; Addy, D. A.; Riddlestone, I.; Kelly, M.; Phillips, N.; Aldridge, S. *J. Am. Chem. Soc.* **2011**, *133*, 11500. (b) Vidovic, D.; Addy, D. A.; Krämer, T.; McGrady, J.; Aldridge, S. *J. Am. Chem. Soc.* **2011**, *133*, 8494.
(31) Douglas, T. M.; Chaplin, A. B.; Weller, A. S. *J. Am. Chem. Soc.* **2008**, *130*, 14432.
(32) Pons, V.; Baker, R. T.; Szymczak, N. K.; Heldebrant, D. J.; Linehan, J. C.; Matus, M. H.; Grant, D. J.; Dixon, D. A. *Chem. Commun.* **2008**, 6597.
(33) Hu, M. G.; Geanangel, R. A.; Wendlandt, W. W. *Thermochim. Acta* **1978**, *23*, 249.
(34) Baumann, J.; Baitalow, F.; Wolf, G. *Thermochim. Acta* **2005**, *430*, 9.
(35) Baitalow, F.; Baumann, J.; Wolf, G.; Jaenicke-Rößler, K.; Leitner, G. *Thermochim. Acta* **2002**, *391*, 159.
(36) Wolf, G.; Baumann, J.; Baitalow, F.; Hoffmann, F. P. *Thermochim. Acta* **2000**, *343*, 19.
(37) Staubitz, A.; Sloan, M. E.; Robertson, A. P. M.; Friedrich, A.; Schneider, S.; Gates, P. J.; Schmedt auf der Günne, J.; Manners, I. *J. Am. Chem. Soc.* **2010**, *132*, 13332.
(38) Vance, J. R.; Robertson, A. P. M.; Lee, K.; Manners, I. *Chem.—Eur. J.* **2011**, *17*, 4099.
(39) Jaska, C. A.; Temple, K.; Lough, A. J.; Manners, I. *Chem. Commun.* **2001**, 962.
(40) Jaska, C. A.; Temple, K.; Lough, A. J.; Manners, I. *J. Am. Chem. Soc.* **2003**, *125*, 9424.
(41) Blaquiere, N.; Diallo-Garcia, S.; Gorelsky, S. I.; Black, D. A.; Fagnou, K. *J. Am. Chem. Soc.* **2008**, *130*, 14034.
(42) Friedrich, A.; Drees, M.; Schneider, S. *Chem.—Eur. J.* **2009**, *15*, 10339.
(43) Jiang, Y.; Berke, H. *Chem. Commun.* **2007**, 3571.
(44) Kawano, Y.; Uruichi, M.; Shimoi, M.; Taki, S.; Kawaguchi, T.; Kakizawa, T.; Ogino, H. *J. Am. Chem. Soc.* **2009**, *131*, 14946.
(45) Baker, R. T.; Gordon, J. C.; Hamilton, C. W.; Henson, N. J.; Lin, P.-H.; Maguire, S.; Murugesu, M.; Scott, B. L.; Smythe, N. C. *J. Am. Chem. Soc.* **2012**, *134*, 5598.
(46) Kim, S.-K.; Kim, T.-J.; Kim, T.-Y.; Lee, G.; Park, J. T.; Nam, S. W.; Kang, S. O. *Chem. Commun.* **2012**, *48*, 2021.
(47) Tang, C. Y.; Phillips, N.; Bates, J. I.; Thompson, A. L.; Gutmann, M. J.; Aldridge, S. *Chem. Commun.* **2012**, *48*, 8096.
(48) Vogt, M.; de Bruin, B.; Berke, H.; Trincado, M.; Grützmacher, H. *Chem. Sci.* **2011**, *2*, 723.
(49) Chapman, A. M.; Wass, D. F. *Dalton Trans.* **2012**, *41*, 9067.
(50) Robertson, A. P. M.; Leitao, E. M.; Manners, I. *J. Am. Chem. Soc.* **2011**, *133*, 19322.
(51) Yang, X.; Zhao, L.; Fox, T.; Wang, Z.-X.; Berke, H. *Angew. Chem., Int. Ed.* **2010**, *49*, 2058.
(52) Hansmann, M. M.; Melen, R. L.; Wright, D. S. *Chem. Sci.* **2011**, *2*, 1554.
(53) Liptrot, D. J.; Hill, M. S.; Mahon, M. F.; MacDougall, D. J. *Chem.—Eur. J.* **2010**, *16*, 8508.
(54) Harder, S.; Spielmann, J. *Chem. Commun.* **2011**, *47*, 11945.
(55) Robertson, A. P. M.; Suter, R.; Chabanne, L.; Whittell, G. R.; Manners, I. *Inorg. Chem.* **2011**, *50*, 12680.
(56) Karahan, S.; Zahmakiran, M.; Özkar, S. *Chem. Commun.* **2012**, *48*, 1180.
(57) Beachley, O. T., Jr. *Inorg. Chem.* **1967**, *6*, 870.
(58) Kimura, T.; Takahashi, T.; Nishiura, M.; Yamamura, K. *Org. Lett.* **2006**, *8*, 3137.
(59) Corey, E. J.; Helal, C. J. *Angew. Chem., Int. Ed.* **1998**, *37*, 1986.
(60) Polshettiwar, V.; Varma, R. S. *Green Chem.* **2009**, *11*, 1313.
(61) Sedelmeier, J.; Ley, S. V.; Baxendale, I. R. *Green Chem.* **2009**, *11*, 683.
(62) Yang, J. W.; Fonseca, M. T. H.; List, B. *Angew. Chem., Int. Ed.* **2004**, *43*, 6660.
(63) Yang, J. W.; Fonseca, M. T. H.; Vignola, N.; List, B. *Angew. Chem., Int. Ed.* **2005**, *44*, 108.
(64) Erős, G.; Nagy, K.; Mehdi, H.; Pápai, I.; Nagy, P.; Király, P.; Tárkányi, G.; Soós, T. *Chem.—Eur. J.* **2012**, *18*, 574.
(65) Rueping, M.; Theissmann, T.; Antonchick, A. P. *Synlett* **2006**, 1071.
(66) Rueping, M.; Antonchick, A. P.; Theissmann, T. *Angew. Chem., Int. Ed.* **2006**, *45*, 3683.
(67) Ouellet, S. G.; Walji, A. M.; Macmillan, D. W. C. *Acc. Chem. Res.* **2007**, *40*, 1327.
(68) Rueping, M.; Sugiono, E.; Schoepke, F. R. *Synlett* **2010**, 852.
(69) Rueping, M.; Sugiono, E.; Schoepke, F. R. *Synlett* **2007**, 1441.
(70) Chase, P. A.; Welch, G. C.; Jurca, T.; Stephan, D. W. *Angew. Chem., Int. Ed.* **2007**, *46*, 8050.
(71) Welch, G. C.; San Juan, R. R.; Masuda, J. D.; Stephan, D. W. *Science* **2006**, *314*, 1124.
(72) Spies, P.; Schwendemann, S.; Lange, S.; Kehr, G.; Fröhlich, R.; Erker, G. *Angew. Chem., Int. Ed.* **2008**, *47*, 7543.
(73) Schulz, F.; Sumerin, V.; Heikkinen, S.; Pedersen, B.; Wang, C.; Atsumi, M.; Leskelä, M.; Repo, T.; Pyykkö, P.; Petry, W.; Rieger, B. *J. Am. Chem. Soc.* **2011**, *133*, 20245.
(74) Sumerin, V.; Chernichenko, K.; Nieger, M.; Leskelä, M.; Rieger, B.; Repo, T. *Adv. Synth. Catal.* **2011**, *353*, 2093.
(75) Yang, X.; Fox, T.; Berke, H. *Org. Biomol. Chem.* **2012**, *10*, 852.
(76) Yang, X.; Fox, T.; Berke, H. *Tetrahedron* **2011**, *67*, 7121.
(77) Zimmerman, P. M.; Zhang, Z.; Musgrave, C. B. *Inorg. Chem.* **2010**, *49*, 8724.
(78) For an early example of a metal-free hydrogenation of an inorganic substrate, see: Spikes, G. H.; Fettinger, J. C.; Power, P. P. *J. Am. Chem. Soc.* **2005**, *127*, 12232.
(79) Recent work in our group suggests $i\mathrm{Pr_2N{=}BH_2}$ reacts with BH_3 to give $[H_2B(\mu\text{-}H)(\mu\text{-}Ni\mathrm{Pr_2})BH_2]$. Robertson, A. P. M; Leitao, E. M.; Manners, I. Unpublished work.
(80) Pasumansky, L.; Haddenham, D.; Clary, J. W.; Fisher, G. B.; Goralski, C. T.; Singaram, B. *J. Org. Chem.* **2008**, *73*, 1898.
(81) Jaska, C. A.; Lough, A. J.; Manners, I. *Inorg. Chem.* **2004**, *43*, 1090.
(82) Stevens, C. J.; Dallanegra, R.; Chaplin, A. B.; Weller, A. S.; MacGregor, S. A.; Ward, B.; McKay, D.; Alcaraz, G.; Sabo-Etienne, S. *Chem.—Eur. J.* **2011**, *17*, 3011.
(83) Sloan, M. E.; Staubitz, A.; Clark, T. J.; Russell, C. A.; Lloyd-Jones, G. C.; Manners, I. *J. Am. Chem. Soc.* **2010**, *132*, 3831.
(84) Estimated values for k_{-2} were employed for runs at 30, 38, and 46 °C; these were obtained from the experimental value for k_{-2} at 22 and 54 °C interpolated via the Eyring equation.
(85) Sewell, L. J.; Lloyd-Jones, G. C.; Weller, A. S. *J. Am. Chem. Soc.* **2012**, *134*, 3598.
(86) Sauer, J.; Sustmann, R. *Angew. Chem., Int. Ed.* **1980**, *19*, 779.
(87) Pathway **3d** via **TS(3d)** is the reverse of the abstraction of BH_3 from $[H_2B(\mu\text{-}H)(\mu\text{-}Ni\mathrm{Pr_2})BH_2]$ by Me_2NH, cf.: (a) Nutt, W. R.; McKee, M. L. *Inorg. Chem.* **2007**, *46*, 7633. (b) Helten, H.; Robertson, A. P. M.; Staubitz, A.; Vance, J. R.; Haddow, M. F.; Manners, I. *Chem.—Eur. J.* **2012**, *18*, 4665.
(88) Additionally, ring-opening reactions of $[H_2B(\mu\text{-}H)(\mu\text{-}Ni\mathrm{Pr_2})BH_2]$ induced by Me_2NH were considered (see Supporting

Information). The calculated barriers of these reactions were significantly higher than that of reaction **1**.
(89) The transition states **TS(3d)** via pathway **4** and **TS(2d)** via pathway **4** could not be located. In constrained searches along the reaction coordinates, the total energy of the system decreased monotonically. This suggests that both pathways should have negligible activation barriers.
(90) With two of the seven computational methods used in a detailed study, a hydrogen-bonded complex between $i\mathrm{Pr_2N{=}BH_2}$ and $\mathrm{Me_2NH{\cdot}BH_3}$ (**pre-1**) was found as a local minimum in energy (see Figure SI-31). However, in these cases, its formation from separated reactants is predicted to be too highly endergonic to constitute a pre-equilibrium preceding hydrogen transfer. As a consequence, if a complex between $i\mathrm{Pr_2N{=}BH_2}$ and $\mathrm{Me_2NH{\cdot}BH_3}$ is formed, it represents a transient intermediate in the course of transfer hydrogenation, and its formation has no effect on the kinetic and thermodynamic parameters of the overall reaction.
(91) Structures of **TS(1)** calculated with other methods are shown in the Supporting Information (Figure SI-32).
(92) Wigner, E. *Phys. Rev.* **1932**, *40*, 749.
(93) Luo, Y.; Ohno, K. *Organometallics* **2007**, *26*, 3597.
(94) Jiang, C.; Blacque, O.; Fox, T.; Berke, H. *Dalton Trans.* **2011**, *40*, 1091.
(95) Jiang, Y.; Blacque, O.; Fox, T.; Frech, C. M.; Berke, H. *Organometallics* **2009**, *28*, 5493.
(96) Vogt, M.; de Bruin, B.; Berke, H.; Trincado, M.; Grützmacher, H. *Chem. Sci.* **2011**, *2*, 723.
(97) Yang, X.; Fox, T.; Berke, H. *Chem. Commun.* **2011**, *47*, 2053.
(98) Sanderson, R. T. *J. Am. Chem. Soc.* **1983**, *105*, 2259.
(99) Westheimer, F. H. *Chem. Rev.* **1961**, *61*, 265.
(100) O'Ferrall, R. A. M. *J. Chem. Soc. B* **1970**, 785.
(101) Pangborn, A. B.; Giardello, M. A.; Grubbs, R. H.; Rosen, R. K.; Timmers, F. J. *Organometallics* **1996**, *15*, 1518.
(102) Frisch, M. J.; Trucks, G. W.; Schlegel, H. B.; Scuseria, G. E.; Robb, M. A.; Cheeseman, J. R.; Scalmani, G.; Barone, V.; Mennucci, B.; Petersson, G. A.; Nakatsuji, H.; Caricato, M.; Li, X.; Hratchian, H. P.; Izmaylov, A. F.; Bloino, J.; Zheng, G.; Sonnenberg, J. L.; Hada, M.; Ehara, M.; Toyota, K.; Fukuda, R.; Hasegawa, J.; Ishida, M.; Nakajima, T.; Honda, Y.; Kitao, O.; Nakai, H.; Vreven, T.; Montgomery, J. A., Jr.; Peralta, J. E.; Ogliaro, F.; Bearpark, M.; Heyd, J. J.; Brothers, E.; Kudin, K. N.; Staroverov, V. N.; Kobayashi, R.; Normand, J.; Raghavachari, K.; Rendell, A.; Burant, J. C.; Iyengar, S. S.; Tomasi, J.; Cossi, M.; Rega, N.; Millam, J. M.; Klene, M.; Knox, J. E.; Cross, J. B.; Bakken, V.; Adamo, C.; Jaramillo, J.; Gomperts, R.; Stratmann, R. E.; Yazyev, O.; Austin, A. J.; Cammi, R.; Pomelli, C.; Ochterski, J. W.; Martin, R. L.; Morokuma, K.; Zakrzewski, V. G.; Voth, G. A.; Salvador, P.; Dannenberg, J. J.; Dapprich, S.; Daniels, A. D.; Farkas, Ö.; Foresman, J. B.; Ortiz, J. V.; Cioslowski, J.; Fox, D. J. *Gaussian 09*, Revision A.1; Gaussian, Inc., Wallingford, CT, 2009.
(103) Adamo, C.; Barone, V. *J. Chem. Phys.* **1999**, *110*, 6158.
(104) Perdew, J. P.; Burke, K.; Ernzerhof, M. *Phys. Rev. Lett.* **1996**, *77*, 3865.
(105) Perdew, J. P.; Burke, K.; Ernzerhof, M. *Phys. Rev. Lett.* **1997**, *78*, 1396.
(106) Ditchfield, R.; Hehre, W. J.; Pople, J. A. *J. Chem. Phys.* **1971**, *54*, 724.
(107) Hehre, W. J.; Ditchfield, R.; Pople, J. A. *J. Chem. Phys.* **1972**, *56*, 2257.
(108) Hariharan, P. C.; Pople, J. A. *Mol. Phys.* **1974**, *27*, 209.
(109) Hariharan, P. C.; Pople, J. A. *Theor. Chem. Acc.* **1973**, *28*, 213.
(110) Gordon, M. S. *Chem. Phys. Lett.* **1980**, *76*, 163.
(111) Francl, M. M.; Pietro, W. J.; Hehre, W. J.; Binkley, J. S.; Gordon, M. S.; DeFrees, D. J.; Pople, J. A. *J. Chem. Phys.* **1982**, *77*, 3654.
(112) Miertuš, S.; Scrocco, E.; Tomasi, J. *Chem. Phys.* **1981**, *55*, 117.
(113) Miertuš, S.; Tomasi, J. *Chem. Phys.* **1982**, *65*, 239.
(114) Pascual-Ahuir, J. L.; Silla, E.; Tuñon, I. *J. Comput. Chem.* **1994**, *15*, 1127.
(115) Cossi, M.; Barone, V.; Cammi, R.; Tomasi, J. *Chem. Phys. Lett.* **1996**, *255*, 327.
(116) Cossi, M.; Barone, V.; Mennucci, B.; Tomasi, J. *Chem. Phys. Lett.* **1998**, *286*, 253.
(117) Cossi, M.; Rega, N.; Scalmani, G.; Barone, V. *J. Chem. Phys.* **2001**, *114*, 5691.
(118) Cossi, M.; Scalmani, G.; Rega, N.; Barone, V. *J. Chem. Phys.* **2002**, *117*, 43.
(119) Barone, V.; Cossi, M.; Tomasi, J. *J. Chem. Phys.* **1997**, *107*, 3210.
(120) Cancès, E.; Mennucci, B.; Tomasi, J. *J. Chem. Phys.* **1997**, *107*, 3032.
(121) Mennucci, B.; Cancès, E.; Tomasi, J. *J. Chem. Phys. B* **1997**, *101*, 10506.
(122) Mennucci, B.; Tomasi, J. *J. Chem. Phys.* **1997**, *106*, 5151.
(123) Tomasi, J.; Mennucci, B.; Cancès, E. *J. Mol. Struct. (Theochem)* **1999**, *464*, 211.